The interaction of ω_2 with the RNA polymerase β' subunit functions as an activation to repression switch

Andrea Volante, Begoña Carrasco, Mariangela Tabone and Juan C. Alonso*
Departamento de Biotecnología Microbiana, Centro Nacional de Biotecnología, CNB-CSIC, 3, Darwin Street, 28049 Madrid, Spain.

Annex 1.

Partial P_ω occupancy by ω_2 activates transcription

Protein ω_2 has a high affinity for operators that contain at least two consecutive heptads. This affinity increases when four or more heptads are involved (K_{Dapp} 5 ± 1) (1). However, with a single heptad or with heptads separated by one or more base pairs, binding is extremely poor (K_{Dapp} > 800 nM) (1). The affinity also depends on heptad organization and is maximal for converging (→←, K_{Dapp} ~20 nM), while lower for direct (→→, K_{Dapp} ~40 nM) and diverging (←→, K_{Dapp} 120 nM) heptad arrangements (1). The ω_2 protein does not distort the DNA structure upon binding to →→ or →← DNA (2). These structures show that a pair of positively charged, antiparallel β strands of ω_2 insert into the major groove of DNA and establish sequence-dependent contacts to symmetric or asymmetric repetitive sequences with a 0.3 Å deviation with respect to the central C-G pair of each repetition (2-5). The interaction between RNAP-σ^A and P_ω DNA was enhanced with sub-stoichiometric concentrations of ω_2 (Fig. 2). We hypothesised that, under these conditions, ω_2 would preferentially bind to heptads with a →← configuration (e.g, heptads 6 and 7) (Fig. S1 and 3A). These heptads overlapped the -35 element and the spacer region (positions -34 to -21). To test this hypothesis, the heptad 6 (←, 5'-TGTGAgT-3'), 7 (←, 5'-TaatcTT-3'), or heptads 6 plus 7 (←←, 5'- TGTGAgTTaatcTT-3') were mutagenized. Run-off transcription experiments were then performed with each. As a control, equivalent mutations were introduced in heptad 1 (→), 2 (→) or heptads 1 plus 2 (→→) (Fig. S1 and 3A). With the exception of mutated sequences of heptads 6 plus 7 (which included mutations within the -35 element), RNAP-σ^A transcribed the P_ω variants nearly as well as the wt in the absence of ω_2 (data not shown). Similar levels of transcription were observed in the presence of limiting or stoichiometric amounts of ω_2. This result suggests that the selective occupancy of heptads 6 and 7 play a minor role, if any, in ω_2 regulation of P_ω utilization.

Annex 2.

Proteins ω_2 or $\omega2_2$ repress P_δ utilization

The ω_2 protein has three functional regions: i) the unstructured NTD (residues 1-19) required for the $\omega_2{\cdot}\delta_2$ interaction (4); ii) the β-sheet domain (residues 28-32), which is necessary for DNA binding (2,3,5); and iii) the α-helix α1 (residues 34-46) which in concert with the α-helix α2 domain (residues 51-64) contribute to monomer-monomer and dimer-dimer interfaces (2,3). Whether or not residues 10-28 and the C-terminal residues 65-71 have anything more than a structural role to play is unknown (3,6).

Members of the superfamily of ω_2 regulators can be divided into two sub-families, of which ω and ω2 are representative (7,8). Monomeric ω2 (79-residues long) shares 98% identity with ω (71-amino acids) within the first 55 residues, but the degree of identity drops to 18% in the remaining 24 residues (Fig. S7A). With the aim of mapping the ω_2 domain involved in the interaction with RNAP-σ^A, and to test whether a similar mechanism of action applies to other ω_2 regulated promoters, we compared P_δ promoter binding and consequent transcription repression activity, *in vivo,* of $\omega2_2$, ω_2 or $\omega_2\Delta$N19, which lacks the 19 first amino acids (4). A single copy of P_δ was fused to the promoter-less *lacZ* gene and integrated into the *amyE* locus of the *B. subtilis* genome as a unique copy. This operation was performed in the BG508 strain (9). This construct was used to measure the effect of these ω-like genes *in trans*. The results of β-galactosidase activity assays showed that ω2 repressed P_δ mediated transcription to levels comparable to those of ω_2 or $\omega_2\Delta$N19 (Fig. S7B) (2,4,9). The suggested that the dimer is the functional form of ω2 and that the different C-terminal domains of ω and ω2 are not involved in gene repression. *In vivo* experiments also revealed an increase in the repression of P_δ utilization in the presence of both ω_2 and δ_2 (Fig. 7B), suggesting that these proteins act in concert.

Annex 3.

The central and C-terminal regions of ω_2 might not interact with RNAP-σ^A

The strain bearing the P_δ:*lac*Z fusion (see *Annex 2*) was transformed with a plasmid carrying a ω sequence that had a mutation either in its coiled (ωK52A), α-helix α2 (ωE53A), or hypothetical α-helix α2' (ωR70A) regions. The effect of these mutants on P_δ expression was comparable to that of wt ω_2 *in trans*. All of them repressed P_δ transcription by >50-fold (Fig. S7B). An intermediate effect was observed with the ωR64A mutant, which repressed P_δ utilization by ~30-fold (Fig. S7B). However, the D56A mutant only reduced P_δ transcription

~6-fold. Since the intracellular concentrations of ω_2 and its mutant variants were similar (data not shown), we tentatively proposed that ω_2D56A was impaired in its interaction with either P_ω DNA, with itself or with RNAP-σ^A. To test these hypotheses, the ωD56A gene was over-expressed and its product was purified and characterized *in vitro*.

In comparison with the wt, the ωD56A protein binds P_ω DNA weakly (data not shown). Also, smaller proportion of this mutant protein assembles into dimers (Fig. S7C). In light of the fact that, in the dimeric form of ω, the β-sheet adopts an antiparallel orientation before binding P_ω DNA, we propose that the main consequence of D56A mutation is poor ω dimerization. This is consistent with the observation that ωD56A binds P_ω DNA with reduced affinity and suggests that D56 contributes to the ω·ω interface (Fig. S7D). Therefore, ωD56A was not analysed further. It would be very interesting to determine whether the ω_2 NTD can by itself recruit RNAP-σ^A to the $\omega_2 \cdot P_\omega$ DNA complex.

References

1. de la Hoz, A.B., Pratto, F., Misselwitz, R., Speck, C., Weihofen, W., Welfle, K., Saenger, W., Welfle, H. and Alonso, J.C. (2004) Recognition of DNA by ω protein from the broad-host range *Streptococcus pyogenes* plasmid pSM19035: analysis of binding to operator DNA with one to four heptad repeats. *Nucl Acids Res*, **32**, 3136-3147.
2. Weihofen, W.A., Cicek, A., Pratto, F., Alonso, J.C. and Saenger, W. (2006) Structures of ω repressors bound to direct and inverted DNA repeats explain modulation of transcription. *Nucl Acids Res*, **34**, 1450-1458.
3. Murayama, K., Orth, P., de la Hoz, A.B., Alonso, J.C. and Saenger, W. (2001) Crystal structure of ω transcriptional repressor encoded by *Streptococcus pyogenes* plasmid pSM19035 at 1.5Å resolution. *J Mol Biol*, **314**, 789-796.
4. Welfle, K., Pratto, F., Misselwitz, R., Behlke, J., Alonso, J.C. and Welfle, H. (2005) Role of the N-terminal region and of β-sheet residue Thr29 on the activity of the ω_2 global regulator from the broad-host range *Streptococcus pyogene*s plasmid pSM19035. *Biol Chem*, **386**, 881-894.
5. Dostál, L., Pratto, F., Alonso, J.C. and Welfle, H. (2007) Binding of regulatory protein ω from *Streptococcus pyogenes* plasmid pSM19035 to direct and inverted 7-Base pair repeats of operator DNA. *J. Raman Spectrosc*, **38**, 166-175.
6. Murayama, K., de la Hoz, A.B., Alings, C., Lopez, G., Orth, P., Alonso, J.C. and Saenger, W. (1999) Crystallization and preliminary X-ray diffraction studies of *Streptococcus pyogenes* plasmid pSM19035-encoded ω transcriptional repressor. *Acta Crystallogr D Biol Crystallogr*, **55 (Pt 12)**, 2041-2042.
7. Lioy, V.S., Pratto, F., de la Hoz, A.B., Ayora, S. and Alonso, J.C. (2010) Plasmid pSM19035, a model to study stable maintenance in Firmicutes. *Plasmid*, **64**, 1-17.
8. Croucher, N.J., Harris, S.R., Fraser, C., Quail, M.A., Burton, J., van der Linden, M., McGee, L., von Gottberg, A., Song, J.H., Ko, K.S. *et al.* (2011) Rapid pneumococcal evolution in response to clinical interventions. *Science*, **331**, 430-434.

9. de la Hoz, A.B., Ayora, S., Sitkiewicz, I., Fernandez, S., Pankiewicz, R., Alonso, J.C. and Ceglowski, P. (2000) Plasmid copy-number control and better-than-random segregation genes of pSM19035 share a common regulator. *Proc Natl Acad Sci U S A*, **97**, 728-733.
10. Miller, J.H. (1972) *Experiments in Molecular Genetics* Cold Spring Harbor Lab. Press, Plainview, NY.

Figure legends

Fig. S1. Protein ω_2 or $\omega2_2$ cognate sites. Illustration of the P_ω, $P_{\omega2}$, $P_{\delta,}$ and $P_{copS/R/F}$ regions from plasmids pIP501[a], pSM19035[b], pAMβ1[c], pRE25[d], and pVEF23[e]. The positions of nucleotides are numbered relative to the transcription start site. Contiguous 7-bp repeats and their relative orientations are represented with either → or ←. The -35 and -10 elements are indicated with rectangles and the transcription start sites indicated with solid arrows bent 90º. The dotted-line rectangles and the empty, bent arrows marked with a "?" denote uncharacterized promoters.

Fig. S2. The ω_2 protein modulates RNAP-σ^A binding to P_ω DNA. The 423-bp [α^{32}P]-P_ω DNA (1 nM) was incubated with a range of concentrations of ω_2 (7.5, 15 and 30 nM in [**A**] or 7.5, 15, 30 to 60 in [**B**]) or concentrations of RNAP-σ^A (3.7, 7.5, 15 and 30 nM in *A* and *B*). Alternatively, the amount of ω_2 was fixed either at 3.7 nM in (*A*, lanes 10-13), 7.5 nM (*B*, lanes 12-16) or 60 nM (B, lanes 17-21) while the concentration of RNAP-σ^A was varied (3.7, 7.5, 15 and 30 nM). After DNase I treatment, the complexes were analysed by dPAGE. The +1 site is labelled in the diagram of the operator site-promoter P_ω region. The dotted-line rectangle in (*A*) highlight the extended footprint of RNAP-σ^A in lanes 8-10.

Fig. S3. Cooperative binding of ω_2, δ_2 and RNAP-σ^A to P_ω DNA. Linear 423-bp [α^{32}P]-*Hin*dIII-*Kpn*I P_ω DNA (0.2 nM) was incubated with either 0.75 or 6 nM of ω_2, either 7.5 or 30 nM of RNAP-σ^A, or 37, 75, or 150 nM of δ_2. Alternatively, the concentration of ω_2 was fixed at 0.75 nM, while a range of concentrations of δ was used (37, 75 and 150 nM). Also tested was a fixed concentration of both ω_2 (0.75 nM) and RNAP-σ^A (7.5 nM) in the presence of a varied amount of δ_2 (37, 75 and 150 nM). These reactions were performed for 15 min at 37 ˚C in buffer C in the presence (**A**) or absence (**B**) of 1 mM ATP. (**C**) P_ω DNA was incubated with increasing amounts of ω_2 (0.75, 1.5, 3, 6, 12 and 24 nM, solid circles) or δ_2-ATP (18.5, 37, 75, 150, 300 and 600 nM, solid squares). Alternatively, ω_2 was fixed (0.75 nM) and increasing amounts of δ_2-ATP (9.2, 18.5, 37, 7.5, 150 and 300 nM, empty squares) used, or apo-δ_2 was fixed (37 nM) and increasing concentrations of ω_2 (0.19, 0.37, 0.75, 1.5, 3 and 6 nM, empty circles) used. The signals present in the protein-DNA complex and in the free-DNA (FD) was determined by densitometry. The data presented here are averages and standard deviations of the results of at least three independent experiments. (*D*) Binding of δ_2 and RNAP-σ^A to P_ω DNA. A 423-bp [α^{32}P] P_ω DNA was incubated with increasing amounts of δ_2 (37, 75 and 150 nM) or RNAP-σ^A (15, 30 and 60 nM), or a fixed concentration of RNAP-σ^A (15, 30 or 60 nM) and increasing concentrations of δ_2 (37, 75, 150, 3 nM) in buffer A containing 1 mM ATP for 15 min at 37° C. The signals present in the protein-DNA complex and in the FD was determined by densitometry.

Fig. S4. Effect of ω_2 on the formation of a RNAP-σ^A-promoter RP_O complex with P_ω DNA. (**A**) 423-bp [α^{32}P]-*Hin*dIII-*Kpn*I P_ω DNA (1 nM) was pre-incubated with increasing concentrations of ω_2 (1.8, 3.5, 7.5, 15, 30 and 60 nM, solid circles). Then, a fixed amount of RNAP-σ^A (7.5 nM) in the absence (lanes 1-8) or presence (lanes 9-16) of the initiating nucleotides GTP and ATP was added. DNA melting was probed by $KMnO_4$ footprinting. The positions hypersensitive to $KMnO_4$ are marked (RP_O and RP_{INIT}) and depicted at the bottom; the coordinates are indicated relative to the transcription start point. Purine (G +A) chemical sequencing reactions are shown. Also depicted are the relevant regions. (**B**) Plot of the relative intensity of the bands of the RP_O and RP_{INIT} hypersensitive sites. Band intensities were determined by densitometry. The data presented here are averages and standard deviations of the results of at least three independent experiments.

Fig. S5. RNAP-σ^A-promoter RP_O at P_ω is not affected by δ_2. 423-bp *Hin*dIII-*Kpn*I P_ω DNA (1 nM) was incubated with a fixed amount of RNAP-σ^A (7.5 nM) in the absence (lane 5) or presence of increasing concentrations of δ_2 (75, 150, 300 and 600 nM) in the presence of the initiating nucleotides (GTP and ATP) and DNA melting (open complex) was probed by KMnO4 footprinting. The positions hypersensitive to KMnO4 are marked (RP_O and RP_{INIT}); the coordinates are indicated relative to the transcription start point. The data presented are representative of at least three independent experiments. Purine (G +A), chemical sequencing reactions are shown. The relevant regions of P_ω are depicted.

Fig. S6. RNAP-σ^A retains ω_2. A mixture containing 1.5 μg His-tagged RNAP-σ^A and of ω_2 in buffer A was loaded onto a 50 μl Ni^{2+} micro-column at room temperature. After extensive washing, the retained proteins were eluted with 50 μl buffer B containing 1 M NaCl and 0.4 M imidazole. These were resolved by SDS-PAGE and stained with Coomassie blue. The data presented are representative of at least three independent experiments.

Fig. S7. Protein $\omega 2_2$ recognizes and represses P_δ utilization. (**A**) Clustal W2 sequence alignment of the transcriptional repressors ω and ω2 with secondary structure elements shown above. The identical and conserved amino acids denoted in red and in blue, respectively. (**B**) Activity specified by P_δ in the presence or absence of the indicated product. The β-galactosidase activity is expressed in Miller units (10). Values presented are the means of data from at least four separate experiments. (**C**) Either wt ω_2 or the ωD56A variant was incubated with increasing concentrations of the DSS cross-linking agents. The proteins were resolved by 12.5% SDS-PAGE and the proportion of protein found in dimers was calculated. (**D**) Structural model of ω_2-bound to P_ω DNA. This is derived from the 3D co-structure of the minimal operator site and $\omega_2\Delta19$ (1IRQ PDB) (2). The position of D56 is highlight in red.

Fig. S8. A model of ω_2 and RNAP-σ^A in a complex with P_ω DNA. Shown is the spatial occupancy model of three ω_2 bound to P_ω in the presence or absence of β' alone or RNAP-σ^A. The modelled structures were prepared with I-Tasser and visualized with PyMOL version 1.5.0.4. The structures of the RNAP subunits of *B. subtilis* are represented using the following colour scheme: the σ factor (green), α^I and α^{II} (orange and light orange), β (blue) and the β' subunit (red). The DNA is indicated in orange and the –35 and –10 sites in yellow. Protein ω_2 is represented in pink and grey.

Fig. S1

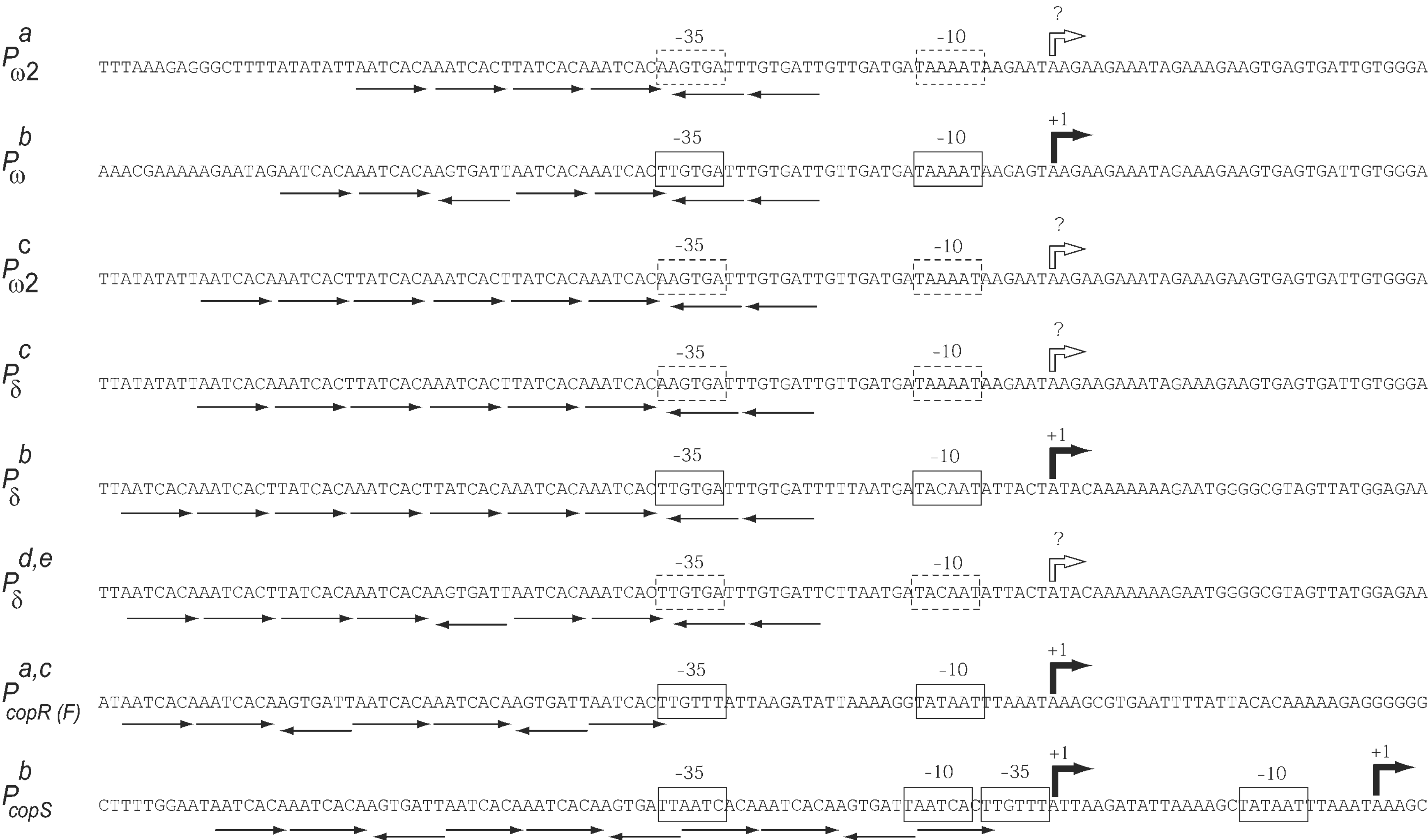

P ω2 a
-35
-10
?
TTTAAAGAGGGCTTTTATATATTAATCACAAATCACTTATCACAAATCACAAGTGATTTGTGATTGTTGATGATAAAATAAGAATAAGAAGAAATAGAAAGAAGTGAGTGATTGTGGGA
P ω b
-35
-10
+1
AAACGAAAAAGAATAGAATCACAAATCACAAGTGATTAATCACAAATCACTTGTGATTTGTGATTGTTGATGATAAAATAAGAGTAAGAAGAAATAGAAAGAAGTGAGTGATTGTGGGA
P ω2 c
-35
-10
?
TTATATATTAATCACAAATCACTTATCACAAATCACTTATCACAAATCACAAGTGATTTGTGATTGTTGATGATAAAATAAGAATAAGAAGAAATAGAAAGAAGTGAGTGATTGTGGGA
P δ c
-35
-10
?
TTATATATTAATCACAAATCACTTATCACAAATCACTTATCACAAATCACAAGTGATTTGTGATTGTTGATGATAAAATAAGAATAAGAAGAAATAGAAAGAAGTGAGTGATTGTGGGA
P δ b
-35
-10
+1
TTAATCACAAATCACTTATCACAAATCACTTATCACAAATCACAAATCACTTGTGATTTGTGATTTTTAATGATACAATATTACTATACAAAAAAAGAATGGGGCGTAGTTATGGAGAA
P δ d,e
-35
-10
?
TTAATCACAAATCACTTATCACAAATCACAAGTGATTAATCACAAATCACTTGTGATTTGTGATTCTTAATGATACAATATTACTATACAAAAAAAGAATGGGGCGTAGTTATGGAGAA
P copR (F) a,c
-35
-10
+1
ATAATCACAAATCACAAGTGATTAATCACAAATCACAAGTGATTAATCACTTGTTTATTAAGATATTAAAAGGTATAATTTAAATAAAGCGTGAATTTTATTACACAAAAAGAGGGGGG
P copS b
-35
-10
-35
+1
-10
+1
CTTTTGGAATAATCACAAATCACAAGTGATTAATCACAAATCACAAGTGATTAATCACAAATCACAAGTGATTAATCACTTGTTTATTAAGATATTAAAAGCTATAATTTAAATAAAGC

Fig. S2

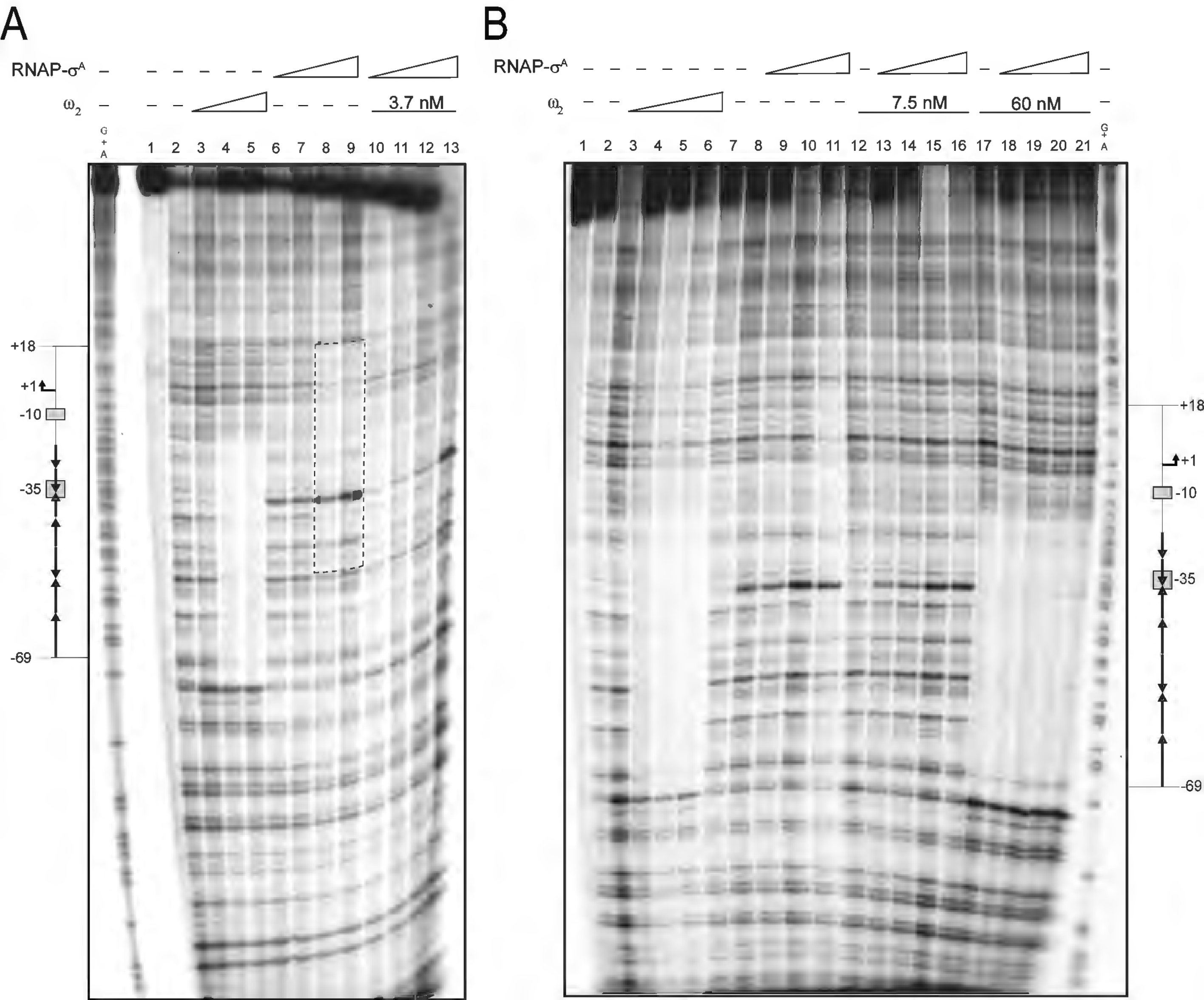
A
RNAP-σ^A
ω2
3.7 nM
G + A
1 2 3 4 5 6 7 8 9 10 11 12 13
+18
+1
-10
-35
-69
B
RNAP-σ^A
ω2
7.5 nM
60 nM
1 2 3 4 5 6 7 8 9 10 11 12 13 14 15 16 17 18 19 20 21
G + A
+18
+1
-10
-35
-69

Fig. S3

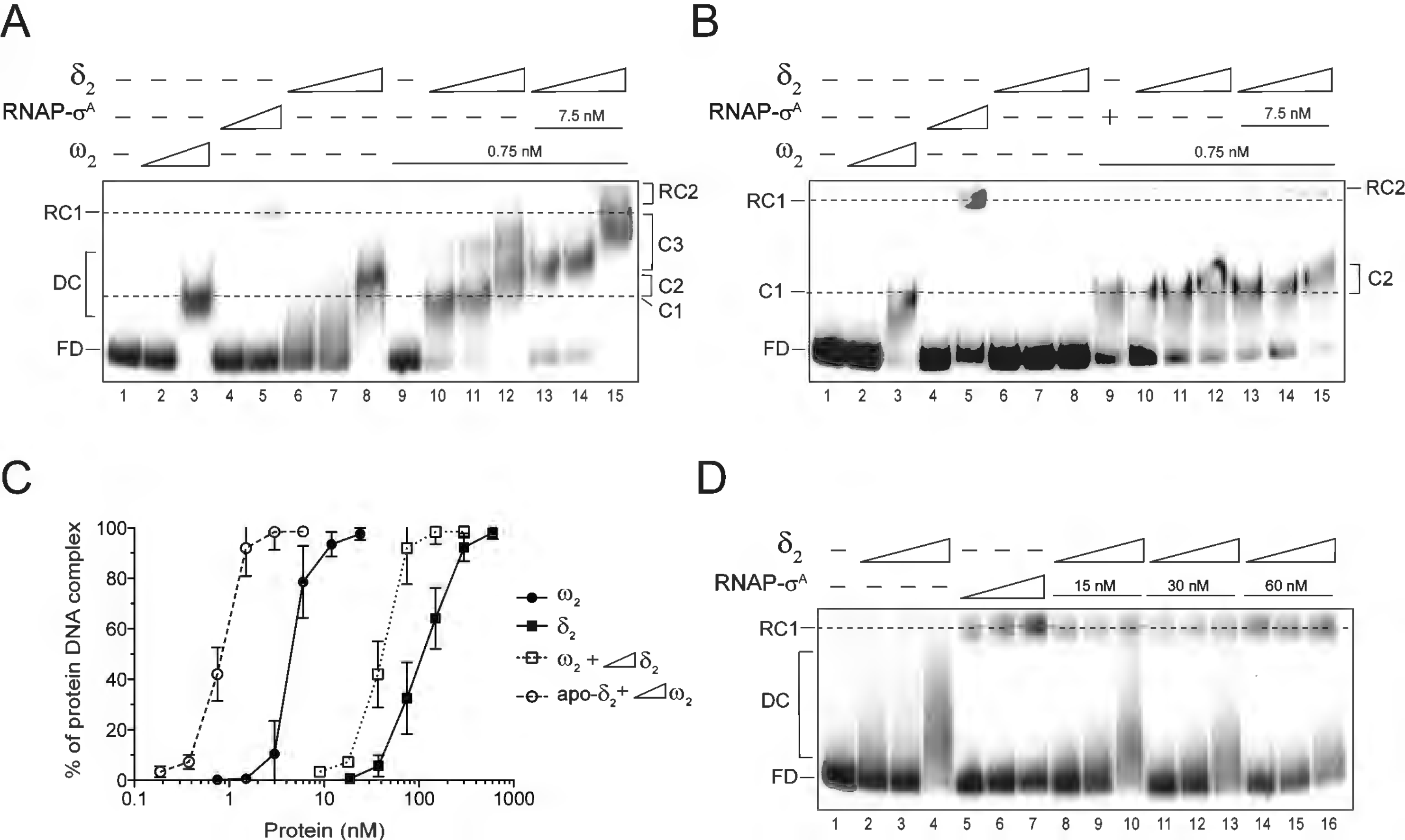

A
δ_2
RNAP-σ^A
7.5 nM
ω_2
0.75 nM
RC1
DC
FD
RC2
C3
C2
C1
1 2 3 4 5 6 7 8 9 10 11 12 13 14 15
B
δ_2
RNAP-σ^A
+
7.5 nM
ω_2
0.75 nM
RC1
C1
FD
RC2
C2
1 2 3 4 5 6 7 8 9 10 11 12 13 14 15
C
% of protein DNA complex
0 20 40 60 80 100
0.1 1 10 100 1000
Protein (nM)
ω_2
δ_2
ω_2 + δ_2
apo-δ_2+ ω_2
D
δ_2
RNAP-σ^A
15 nM
30 nM
60 nM
RC1
DC
FD
1 2 3 4 5 6 7 8 9 10 11 12 13 14 15 16

Fig. S4

A

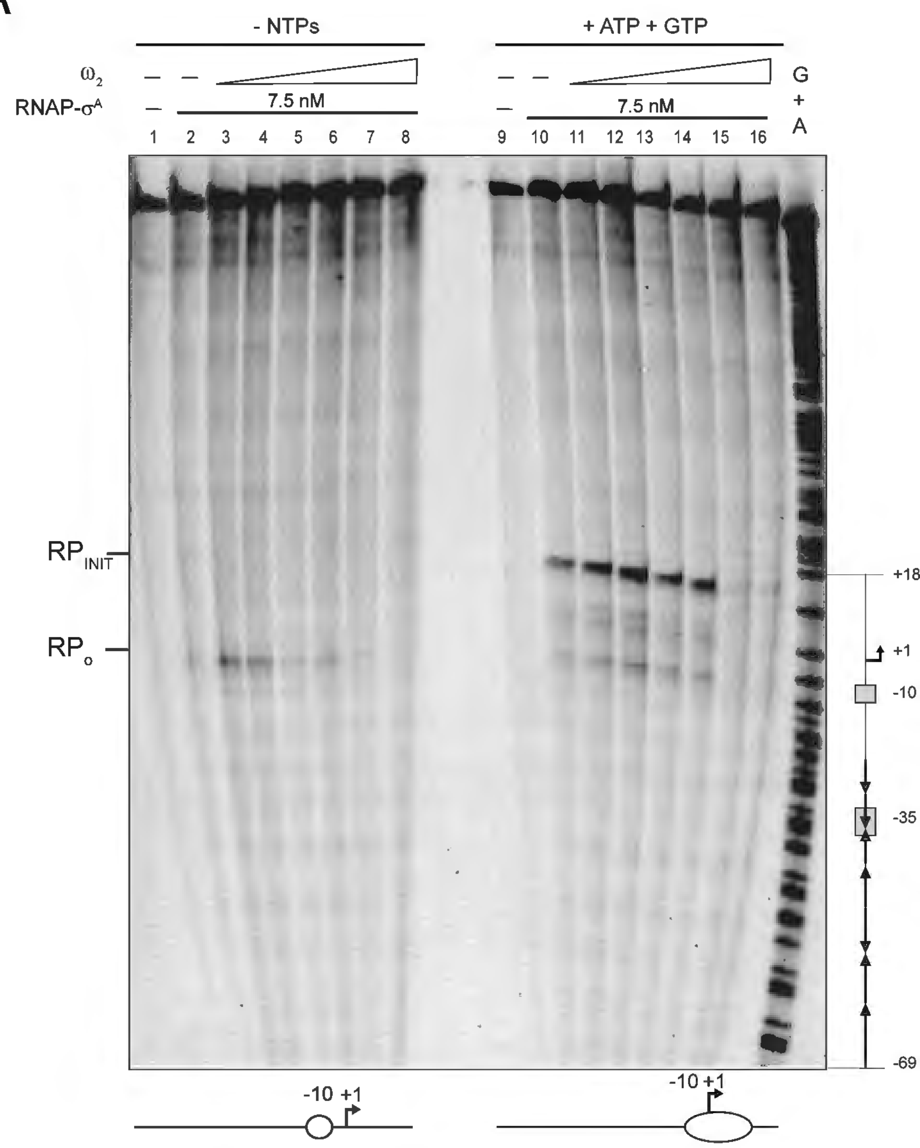
- NTPs
+ ATP + GTP
ω2
RNAP-σA
7.5 nM
7.5 nM
1 2 3 4 5 6 7 8
9 10 11 12 13 14 15 16
G + A
RPINIT
RPo
+18
+1
-10
-35
-69
-10 +1
-10 +1

B

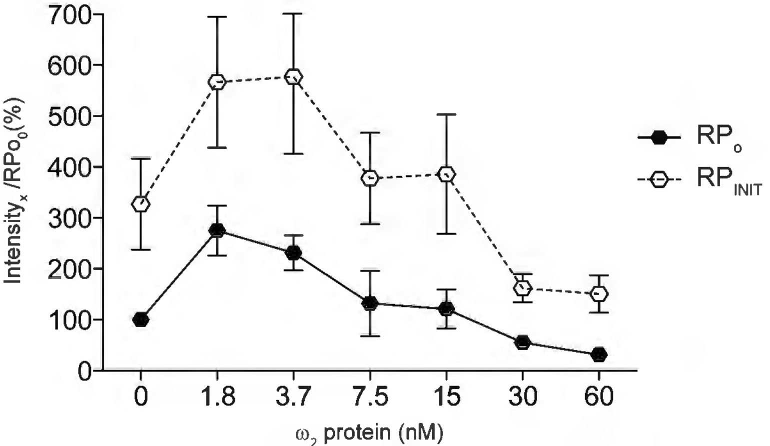
700
600
500
400
300
200
100
0
Intensityx /RPo0(%)
0 1.8 3.7 7.5 15 30 60
ω2 protein (nM)
RPo
RPINIT

Fig. S5

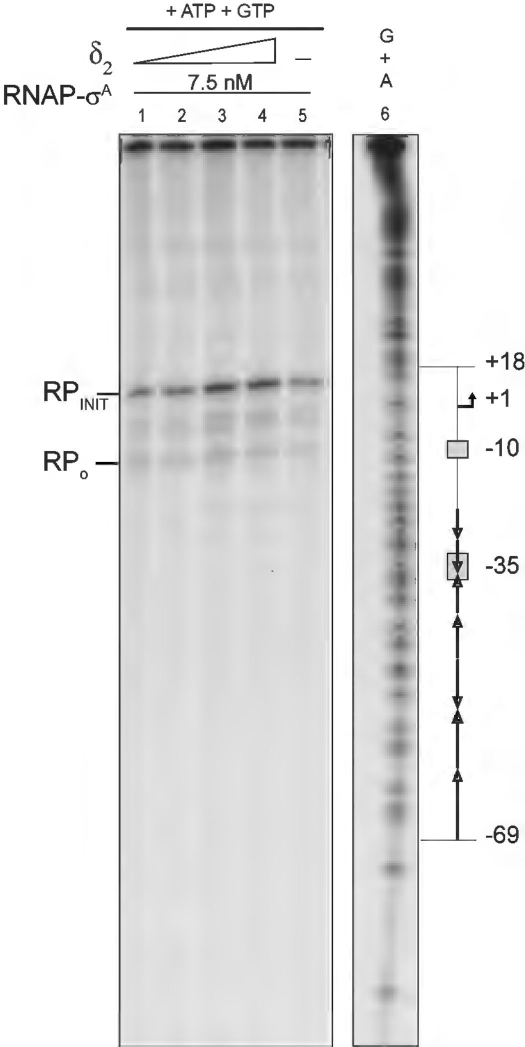

+ ATP + GTP
δ_2
—
RNAP-σ^A
7.5 nM
G
+
A
1
2
3
4
5
6
RP$_{INIT}$
RP$_o$
+18
+1
-10
-35
-69

Fig. S6

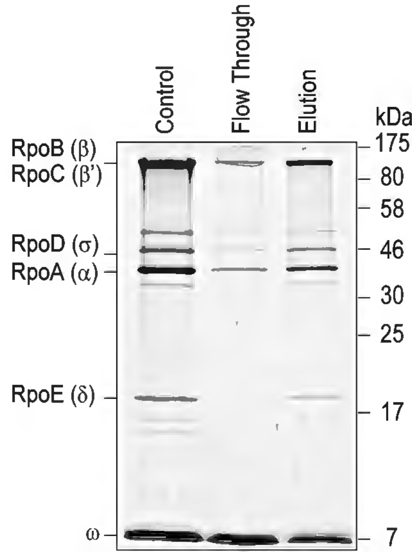
Control
Flow Through
Elution
kDa
175
80
58
46
30
25
17
7
RpoB (β)
RpoC (β')
RpoD (σ)
RpoA (α)
RpoE (δ)
ω

Fig. S7

A

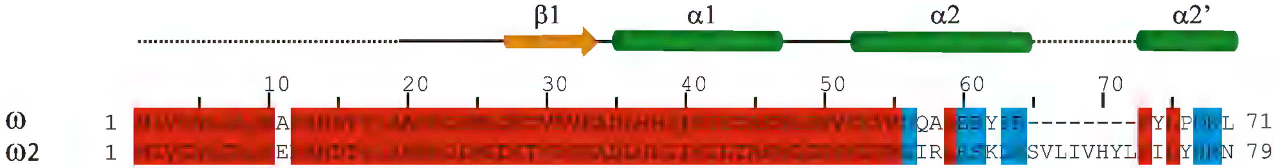

B

Gene in trans	β-Galactosidase activity P_{δ}
none	2317 ± 22
ω	32 ± 12
ω δ	20 ± 8
ω*ΔN19*	44 ± 15
ω*2*	55 ± 14
ω*K52A*	46 ± 9
ω*E53A*	41 ± 8
ω*D56A*	411 ± 42
ω*R64A*	80 ± 9
ω*R70A*	46 ± 9

C

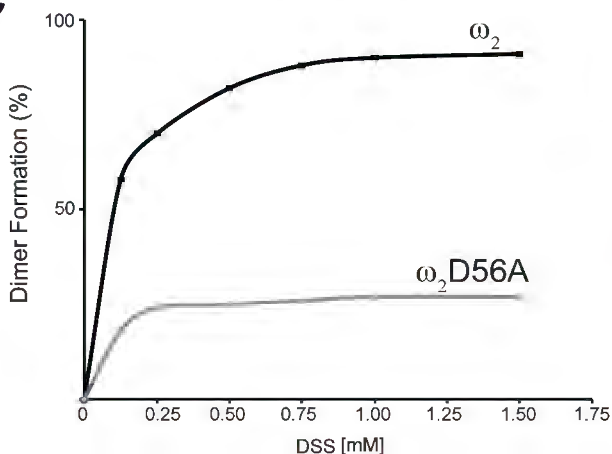

D

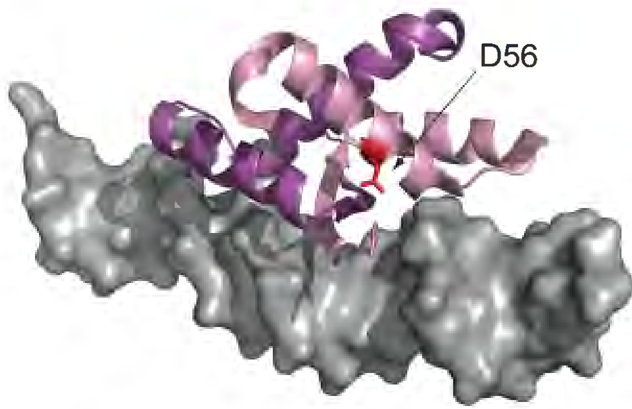

Fig. S8